UC San Diego
UC San Diego Previously Published Works

Title
Engineering of spectator glycocalyx structures to evaluate molecular interactions at crowded cellular boundaries

Permalink
https://escholarship.org/uc/item/3570s8sp

Journal
Faraday Discussions, 219(0)

ISSN
1359-6640

Authors
Honigfort, Daniel J
Zhang, Michelle H
Verespy, Stephen
et al.

Publication Date
2019-10-30

DOI
10.1039/c9fd00024k

Peer reviewed

Engineering of spectator glycocalyx structures to evaluate molecular interactions at crowded cellular boundaries.

Daniel J. Honigfort[a], **Michelle H. Zhang**[a], **Stephen Verespy III**[a,†], **Kamil Godula**[*,a]

[a.]Department of Chemistry and Biochemistry, University of California San Diego, 9500 Gilman Drive, La Jolla, CA 92093-0358, USA

Abstract

In the mucosal epithelium, the cellular glycocalyx can project tens to hundreds of nanometers into the extracellular space, errecting a physical barrier that provides protective functions, mediates the exchange of nutrients and regulates cellular interactions. Little is understood about how the physical properties of the mucosal glycocalyx influence molecular recognition at the cellular boundary. Here, we report the synthesis of PEG-based glycopolymers with tunable glycan composition, which approximate the extended architecture of mucin glycoproteins, and tethered them to the plasma membranes of red blood cells (RBC) to construct an artificial mucin brush-like glycocalyx. We evaluated the associatin of two lectins, ConA and SNA, with their endogenous glycan ligands on the surface of the remodelled cells. The extended glycocalyx provided protection against agglutination of RBCs by both lectins; however, the rate and magnitude of ConA binding were attenuated to a greater degree in the presence of the glycopolymer spectators than those measured for SNA. The different sensitivity of ConA and SNA to glycocalyx crowding likely arises from the distinct presentation of their mannoside and sialoside receptors, respectively, within the native RBC glycocalyx.

Graphical Abstract

Membrane engineering with bystander glycocalyx structures reveals altered protein-receptor association in crowded cell surface environments.
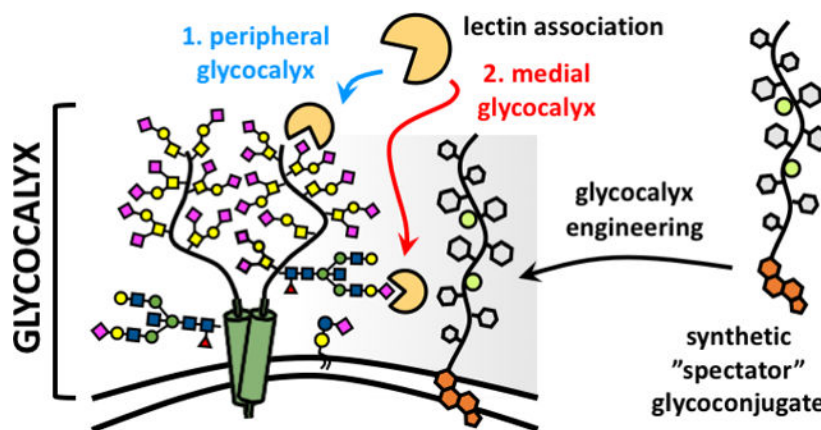
[*]corresponding author (kgodula@ucsd.edu).

[†]Current address: Encodia, Inc. 11125 Flintkote Ave., Suite B, San Diego, CA 92121

Conflicts of interest

There are no conflicts to declare.

Introduction

The cellular glycocalyx is a dynamic carbohydrate-rich macromolecular system populating the boundary between a cell and its surroundings.[1] It is composed of glycolipids and glycoproteins, which can extend tens to hundreds of nanometers above the plasma membrane, providing cells with a physical protective barrier while also facilitating cellular interactions with its environment (Fig 1). The glycan structures distributed throughout the glycocalyx are recognized by a wide array of glycan binding proteins (GBPs), including adhesion molecules found in the extracellular matrix and on neighboring cells, lectins and antibodies of the immune system, or signaling proteins such as growth factors and cytokines. [2] The organization of glycans within glycoconjugates into multivalent ensembles overcomes the characteristically weak binding between individual glycans and their protein partners and produces molecular patterns within the glycocalyx that elicit high-avidity recognition by GBPs.[3]

Macromolecular glycoconjugates isolated from natural sources[4] or generated synthetically[5] have provided important tools for investigating and formulating the paradigms that define our current understanding of how avidity in glycan-protein interactions is achieved.[6] Employed as soluble ligands or integrated into glycan arrays, surface plasmon resonance or biolayer interferometry platforms, synthetic materials (e.g., glycoclusters, spherical glycodendrimers, or linear glycopolymers) have provided key insights into how ligand parameters, such as glycan valency and spacing or scaffold architecture, influence GBP binding and higher-order association (e.g., oligomerization or crosslinking).[7,8] More recently, cell surface engineering approaches have begun to emerge that allow for the integration of these materials directly into the glycocalyx of cells,[9] to further evaluate how the compositional heterogeneity, dynamics and nanoscale organization of the glycocalyx influence biological interactions at the cell surface.

While most work in this area has focused primarily on introducing constellations of specific glycan structures within the glycocalyx and evaluating their recognition by cognate receptors, the effects of the bulk properties of the glycocalyx on cellular interactions and functions are also becoming increasingly pursued. For instance, the remodelling of plasma membranes of mammary epithelial cells with lipidated glycopolymer mimetics of mucin glycoproteins was found to exert biomechanical forces that promoted the assembly of integrin adhesion complexes and enhanced signaling associated with cell proliferation, thus identifying a glycocalyx-dependent mechanism for enhancing the survival and metastatic potential of circulating tumor cells.[10] Further studies using more minimalistic models of bulky glycocalyx components (i.e, linear polyethylene glycol and hyperbranched polyglycerol polymers) covalently grafted to membrane proteins of red blood cells (RBCs) afforded shielding of ABO antigens and protection from complement-mediated cell lysis according to polymer size[11,12] and localization within the glycocalyx.[13]

Despite these advances, systematic surveys of the influence of the "spectator" components of the cellular glycocalyx, with respect to the composition, physical properties and organization of glycans, on molecular recognition events at the cell surface are still lacking. Here, we report the synthesis of well-defined linear poly(ethylene glycol) (PEG) backbones that approximate the architecture and properties of mucin glycoproteins and their use for the scaffolding of spectator glycocalyx structures with varied monosaccharide composition at the surfaces of RBCs. The resulting mucinous glycocalyx models exerted differential effects on lectin association with imbedded endogenous glycan receptors according to the structure of the spectator glycoconjugate and lectin identity.

Results and Discussion

Synthesis of mucin-mimetic glycocalyx building blocks.

We initiated our study by establishing a synthetic strategy to generate glycopolymer structures that exhibit key architectural features of mucin glycoproteins while allowing for the facile introduction of a range of glycan structures. Mucins are large, heavily glycosylated proteins populating the surfaces of epithelial cells, and are composed of characteristic variable number tandem repeat regions with a high frequency of *O*-glycosylation sites.[14] The close packing of glycans along the polypeptide chain forces the protein into an extended conformation with high persistence lengths.[15] This property of mucins can be recapitulated in synthetic linear glycopolymers by controlling the positioning of glycan appendages in sufficient density and close proximity to the polymer backbone.

The Bertozzi group has developed two mucin-mimetic polymer architectures based on glycosylated poly(methylvinyl ketone) (pMVK) and poly(serine) scaffolds generated by the controlled reversible addition-fragmentation chain transfer (RAFT)[16] and the ring-opening *N*-carboxyanhydride (NCA)[17] polymerization techniques, respectively. Both approaches afforded functional mucin-like polymeric structures with distinct advantages and drawbacks. While the pMVK scaffold allows for post-polymerization modification with a wide array of glycan structures, its utility is somewhat limited due to the hydrophobicity of the core polyhydrocarbon backbone, which at low glycan content may give rise to amphiphilic

behaviour. The polypeptide-based approach obviates this problem; however, it necessitates the synthesis and purification of glycosylated NCA monomers, which can be challenging.

We decided to address these challenges by building mucin mimetics on hydrophilic PEG scaffolds suitably modified to allow for later stage introduction of glycans, as well as additional functional elements such as surface anchors and optical probes for characterization. We decided to target a set of glycopolymers displaying the monosaccharides glucose (Glc), galactose (Gal), fucose (Fuc), and glucuronic acid (GlcA) (Fig 2A). The sugars were selected based on their common presence in mammalian glycans and their distinct chemical and physical properties. For instance, Glc and Gal share the same molecular composition, but differ in the orientation of the C4 hydroxyl group, which may impact their packing along the polymer chain. In addition, the increased hydrophobicity of Fuc compared to Glc and Gal (logP values of −2.02, −3.24 and −3.38, respectively) and the negative charge of GlcA at physiological pH (pKa = 3.2), may differentially affect the persistence length and physical properties of the resulting glycopolymers.

Using a monomer-activated anionic ring opening polymerization developed by Carlotti and colleagues,[18] we have synthesized an azide-terminated poly(epichlorohydrin) (pECH) polymer (**1**, Fig 2A) with well-defined size (Mn = 43,400 Da, DP ~450) and narrow chain-length distribution (= 1.20). Although the use of a racemic epichlorohydrin monomer produces an atactic pECH polymer **1**, we reasoned that the stereochemical relationships of the pendant sidechains would not significantly impact the overall architecture and physical properties of the desired mucin mimetic glycopolymers. The polymeric precursor **1** was elaborated into fluorescent cell surface-targeting mucin mimetics in a three-step synthetic sequence (Fig 2A). First, we introduced a hydrophobic anchor for plasma membrane targeting via the copper-catalysed alkyne-azide cycloaddition (CuAAC)[19] between the chain-end azide group in **1** and an alkynyl cholestanone derivative **2**[20] (11.0 equiv. per chain-end azide). Treatment of the chloromethyl sidechains in the cholestanone modified pECH polymer **3** with sodium azide[21] (2.0 equiv. per Cl) generated a reactive polymer intermediate **4** primed for a sequential CuAAC conjugation of alkynyl fluorophores (Cy5, ~ 0.5 % sidechains) and propargyl glycosides to complete the desired glycopolymers **5** (Fig 2A). ^{1}H NMR spectroscopy and size exclusion chromatography (SEC) analyses of polymeric intermediate **4**, confirmed quantitative azide-chloride replacement without any observable increase in polymer dispersity (Fig 2B and Fig S8). The levels of fluorophore labelling in glycopolymers **5** were assessed based on UV-VIS absorption profiles and matched values predicted based on reaction stoichiometry. The efficiency of glycan conjugation to the polymer was difficult to establish accurately based on ^{1}H NMR spectroscopy alone, due to the overlap between glycan and polymer proton signals; however, IR spectroscopy analysis of glycopolymers **5** revealed the disappearance of the characteristic azide stretching absorption frequency at $\upsilon = 2100$ cm^{-1} (Fig S17) after conjugation, indicating quantitative side-chain modification.

We anticipated that the close positioning of the pendant glycan residues with respect to the polymer backbone would force the glycopolymers into an extended conformation. This behaviour is supported by aqueous SEC analysis of polymers **5** exhibiting significantly increased retention on the stationary phase compared to a PEO standard of similar molecular

weight (Fig 2C, $M_{w, PEO}$ = 122 kDa). Atomic force microscopy (AFM) of glycopolymers carrying larger lactose disaccharide residues to facilitate visualization provided direct evidence for extended polymer structures (Fig 2D and Fig S18). We were able to clearly observe individual glycopolymer molecules with length distributions measured at 41 ± 6 nm (Fig 2D) confirming that the new glycopolymer architecture can mimic the nanoscale topology of native mucins.

Generation of spectator glycocalyx structures on RBCs

Molecular recognition events at the cell surface occur in the context of the glycocalyx, which often defines the properties of the surrounding microenvironment, such as polarity, pH, permittivity, and crowding, that may influence the energetics of binding as well as molecular diffusion and transport. However, these properties of the glycocalyx environment are rarely considered when evaluating molecular interactions at the cell surface, despite observations that, for instance, the concentrations of the negatively charged sialic acids in the glycocalyx of B cells can reach ~ 100 mM[22] or that transmembrane epithelial mucins produce dense glycoprotein brushes spanning lengths up to ~1,500 nm.[23]

Some of these conditions can be modelled in a controlled fashion at the surfaces of cells by augmenting their endogenous glycocalyx with synthetic glycomaterials. For instance, glycopolymers affixed to the outer leaflet of the plasma membrane via a lipid anchor and exhibit dynamic behaviour, such as lateral membrane diffusion and spatial reorganization in response to cell adhesion forces,[9,10] and to display molecular recognition motifs to promote cell-cell interaction and intra-cellular signalling.[24] We set out to construct a synthetic glycocalyx on the surfaces of RBCs to model the barrier functions of the mucinous epithelial glycocalyx using glycopolymers **5** (Fig 3A). RBCs offer a practical choice for this purpose, due to their relatively modest glycocalyx, which extends less than 10 nm above the plasma membrane, the lack of active endocytosis preventing the uptake and clearance of the exogenously added materials, and their amenability to a range of protein-binding assays.

The treatment of RBCs with Cy5-labelled glycopolymers **5** (c_{pol} = 115 nM - 10.0 μM), resulted in a dose-dependent membrane incorporation of the polymers based on flow cytometry analysis (Fig 3A). Incubation of RBCs with **5-Glc** lacking the cholestanone anchor gave no appreciable cell-surface incorporation of the glycopolymer (Fig S20), indicating that the synthetic introduction of the anchor into the glycopolymers via precursor **3** is successful and necessary for their plasma membrane insertion. As anticipated, the polyanionic GlcA-modified polymer exhibited lower membrane grafting efficiency (~65%) at the highest polymer concentration (10.0 μM) compared to **5**-Glc and **5**-Gal polymers. Interestingly, we also observed somewhat decreased (~12%) grafting for the polymer bearing fucose (**5-Fuc**), which is a more hydrophobic C6-deoxy analogue of L-galactose (Fig 3B). Visual inspection of the remodelled RBCs in a 96 well plate indicated a decreased ability of cells treated with the non-ionic Glc, Gal and Fuc glycopolymers to settle to the bottom of the wells starting at polymer concentrations of ~ 1.8, 3.2, and 5.6 μM, respectively (Fig S22). We saw no changes in sedimentation properties for RBCs treated with the polyanionic **5**-GlcA polymer over the entire range of concentrations (115 nM - 10.0 μM). These observations are consistent with prior findings showing that increasing the size and

surface density of non-ionic polymers, such as methoxypolyethylene glycol (mPEG), covalently grafted to proteins on RBCs resulted in the shielding of cell surface charge and prevented cell sedimentation and plasma protein-induced cell stacking (Rouleaux formation).[11]

Increasing the surface density of the mucin-mimetic glycopolymers on RBCs may introduce membrane deformations due to entropic pressures resulting from mushroom to brush transitions in the compressing polymer brush.[25] Indeed, we observed visible rounding of RBCs at polymer concentrations above 2.5 μM with signs of membrane disintegration in cells treated with 10.0 μM polymers using optical microscopy (Fig 3B and Fig S21). To exclude contributions from altered membrane morphologies to protein binding in the engineered glycocalyx structures, we imaged the remodelled cells using scanning electron microscopy (SEM, Fig 3C). We observed no significant effects on cell shape or membrane structures for polymer treatments at concentrations up to 2.5 μM and confirmed the breakdown of RBCs at 10.0 μM polymer concentration (Fig 3C).

Our analyses indicate that RBCs can be effectively remodelled with mucin mimetics **5** to introduce synthetic glycocalyx structures to the cell surface. The efficiency of polymer incorporation and the resulting physical properties of the remodelled RBCs were strongly influenced by the structure of the monosaccharide component in **5,** and too high polymer density at the plasma membrane ($c_{pol} > 2.5$ μM) led to observable rounding of cells and an eventual cell lysis. Based on these findings, we identified an optimal polymer concentration of 2.5 μM for RBC remodelling, which provides maximal polymer incorporation without adverse effects on membrane morphology.

Effects of spectator glycocalyx structures on lectin interactions with RBCs

The influence of the compositional heterogeneity and organization of the glycocalyx microenvironment on ligand-receptor interactions at the cell surface have recently been drawing attention, as glycans are increasingly considered for therapeutic targeting.[26] For instance, glycan array screens have identified avidity enhancements for the binding of anti-glycan antibodies in the presence of neighboring non-binding glycan epitopes.[27,28] Similarly, ABH blood group antigens presented on the extracellular domains of band 3 proteins on RBCs have been found to modulate the binding of proteins, such as the *Sambucus nigra* agglutinin (SNA) or the human Siglec-2, to sialic acid receptors primarily carried by glycophorins (Fig 1).[29] The localization of the A and B antigens either to the periphery or the center of sialylated glycoprotein clusters in the RBC membranes, respectively, resulted in a differential stabilization of sialoglycan patches and changes in their binding avidity toward SNA and Siglec-2. The phenomenon of glycan clustering is not limited to RBCs and has been found to contribute to a range of biological processes, including host pathogen interactions, tumor antigen recognition and T-cell activation via a mucinous glycosynapse.[30] The mucin-rich glycocalyx covering epithelial cells is believed to provide a semi-permeable physical barrier limiting the diffusion of proteins and particulates to the cell surface and protecting membrane protein structures from chemical and enzymatic degradation.[14] Mucins contribute directly to the organization of glycocalyx structures and drive the clustering of cell adhesion molecules by exerting forces against the surrounding

extracellular environment.10 We set out to evaluate how the presence of a mucin-like glycocalyx brush at the cell surface would influence the interactions of lectins with endogenous glycan receptors. We selected two lectins, Concanavalin A (ConA) and SNA, for their respective specificity in the targeting of two distinct glycan classes prominently represented in the RBC glycocalyx, the oligomannose core of *N*-linked glycans found primarily on band 3, and to a smaller extent, on glycophorins, and the α2,6-linked sialic acids displayed prominently at terminal positions of *O*-linked glycans on glycophorins and glycosphingolipids.

First, we investigated the ability of glycopolymers **5** to protect against RBC agglutination with both lectins. Using agglutination assays with non-remodeled RBCs, we identified the minimal lectin concentrations (c_{agg}) required to induce cell crosslinking and aggregation (Fig S23 and Fig S24). SNA showed ~ 17-fold greater agglutination capacity ($c_{agg,SNA}$ = 33.0 ng/mL) compared to ConA ($c_{agg,ConA}$ = 0.57 μg/mL). This may, presumably, be due to the greater number and accessibility of sialic acid modifications within the glycocalyx compared to the *N*-linked core mannose structures targeted by ConA.

We next examined the ability of polymers **5** to shield RBCs from agglutination by SNA and ConA by determining the changes in the minimal agglutination concentration, (c_{agg}), required for each lectin to agglutinate RBCs remodeled with polymers **5** (c_{pol} = 2.5 μM, (Table 1, Figs S23 and S24). All glycopolymers **5** provided protection against agglutination by both lectins in the following order: Glc < Gal ~ Fuc < GlcA (Table 1). It should be noted that the polyanionic glycopolymer, **5**-GlcA, afforded the most shielding effect (3- to 4-fold increase in c_{agg}), despite its lower density in the glycocalyx (~65% surface grafting efficiency of the non-ionic polymers, **5**-Glc and **5**-Gal, Fig S19). Each polymer within the set showed similar level of shielding against agglutination by both lectins, as measured by the relative change in c_{agg} with respect to non-remodeled cells. This suggests that the bulk properties of the spectator glycocalyx rather than lectin identity provides the dominant contribution toward protection against agglutination in these experiments. Thus, all polymers established a physical barrier against crosslinking with additional repulsive forces arising from increased negative charge density at the surface of cells presenting the glucuronic acid polymer, **5**-GlcA.

These observations led us to investigate whether the spectator glycoconjugates might exert an influence on lectin association within the glycocalyx at sub-agglutination concentrations. Using a flow-cytometry assay, we measured the binding of ConA and SNA to the remodeled RBCs (Fig 4). At ConA and SNA concentrations of 8 ug/mL and 1 ug/mL, respectively, saturation binding was attained for both lectins in ~ 600 sec without any apparent cell aggregation. We observed 7–13% and 6–9% decrease in the total amount of bound ConA and SNA, respectively, at saturation in the presence of polymers **5** compared to untreated control cells (Fig 4). Distinct from the results obtained from hemagglutination experiment, the structure of the glycan appendages in glycopolymers **5** had no significant impact on the magnitude of inhibition of lectin binding; however, all polymers appeared to inhibit ConA binding to the RBC surface to a greater extent compared to SNA.

Analysis of the linear regions of the binding curves revealed ~ 6–10% decrease in initial rates for the association of ConA in the presence of the polymers compared the non-remodelled RBCs (Fig 4 and Fig S26). In contrast, the initial rates for SNA association in the presence of all polymers **5** were indistinguishable from those observed in control cells (Fig 4 and Fig S26), with differences beginning to appear at a later time closer to the point of saturation binding.

Collectively, these observations indicate distinct influence of the spectator glycocalyx on the association of the two lectins (Fig 5). The ConA lectin targets the less accessible mannoside residues of *N*-linked glycans placed in close proximity to the polypeptide chains of glycoproteins and generally positioned deeper within the glycocalyx. As such, the lectin diffusion into the glycocalyx and binding to its glycans is likely to be more sensitive to the presence of crowding spectator glycoconjugates. This is reflected in the initial rates of ConA binding to RBCs in the presence of glycopolymers **5**, and the greater decrease in the total amount of ConA bound at saturation. In contrast, the SNA lectin targets the outermost sialic acid residues in both *N*- and *O*-linked glycans, which are prominently displayed at the periphery of the glycocalyx and, thus, more accessible. As such, the spectator glycoconjugates would not be expected to interfere with SNA binding until all available peripheral glycans are occupied and the diffusion of the lectin deeper into the glycocalyx is required for additional binding. The observed rapid onset of SNA binding with initial rates indistinguishable between polymer-remodeled RBCs and untreated controls followed by spectator-induced inhibition of binding at a later timepoint supports this model. As the binding of the lectins reaches saturation, the effects of the spectator glycocalyx would be expected to become exacerbated due to the increasing crowding from the newly introduced proteins.

Conclusions

In this paper, we have described a new synthetic route to generate glycopolymer mimetics of mucin glycoproteins with well-defined architectures and tuneable glycosylation. Using a non-covalent cell membrane engineering approach, we have delivered these materials to the surfaces of red blood cells to augment the physical properties of their glycocalyx and evaluated the effect of increased molecular crowding on lectin recognition of endogenous glycan receptors. While the polymers attenuated the binding of both lectins near saturation, only the initial rates of ConA association were affected due to increased glycocalyx crowding in the presence of the synthetic glycoconjugate spectators. The unequal sensitivity of ConA and SNA can be rationalized based on the differential accessibility of their respective glycan targets within the glycocalyx.

Methods

Materials

All chemicals, unless stated otherwise, were purchased from Sigma Aldrich and used as received. Reaction progress was checked by analytical thin-layer chromatography (TLC, Merck silica gel 60 F-254 plates) monitored either with UV illumination, or by staining with iodine, ninhydrin, or CAM stain. Solvent compositions are reported on a volume/volume

(v/v) basis unless otherwise noted. Alkynyl cholestanone **2**,[20] and Glc,[31] Gal,[31] Fuc,[32] GlcA,[33] and Lac[34] propargyl glycosides were prepared according to published procedures. Turkey Red Blood Cells as a 10% solution were obtained from Lampire Biological Laboratories (cat # 724908). *Sambucus nigra* agglutinin (SNA) and Concanavalin A (ConA) lectin were purchased from Vector Labs. Fluorescein (FL)-NHS for lectin labeling was purchased from Thermo Scientific and Cyanine 5 (Cy5)-alkyne for labeling of polymers was obtained from Sigma Aldrich (fluorophore structures are shown in SI on page S4). Lectins were labeled according to manufacturer protocols and the extent of labeling and lectin concentration was adetermined by UV-VIS spectroscopy and BCA assay, respectively. A detailed list of analytical instruments and general procedures used for the purification and structural characterization of synthetic materials and for polymer and cell imaging (optical microscopy, AFM, and SEM) can be found in the Supporting Information.

Synthesis of azide-terminated poly(epichlorohydrin), pECH (1)

Epichlorohydrin was polymerized according to the procedure developed by Carlotti.[18] Briefly, a flame-dried Schlenk flask (10mL) equipped with a magnetic stirrer and fitted with PTFE stopcock was charged with tetrabutylammonium azide (TBAN$_3$, 20 mg, 0.037 mmol, 0.002 equiv.) under argon. A solution of freshly distilled epichlorohydrin (1.29 mL, 16.5 mmol) in anhydrous toluene (4 mL). A solution of triisobutylaluminum in toluene (1.07 M, 104 μL, 0.111 mmol, 0.007 equiv.) was added via a syringe under argon at −30 °C. The reaction was stirred for 4 hours and then stopped by the addition of ethanol. The resulting pECH polymer **1** was precipitated into hexanes and dried under vacuum to yield a clear viscous oil (1500 mg, 99 % yield). The polymer was analyzed by SEC (0.2% LiBr in DMF): $M_w = 52,000$, $M_n = 43,400$, = 1.20).

Synthesis of cholestanone-terminated poly(epichlorohydrin) (3)

In a flame-dried Schlenk flask (10 mL), pECH polymer **1** (15 mg, 0.3 μmol) was dissolved in degassed anhydrous DMSO (200 μL). Alkynyl cholestanone **2** (1.7 mg, 3.8 μmol, 11.0 equiv.) was added, followed by CuI (~0.05mg, 0.3 μmol, 1.0 equiv.) and one drop diisopropylethyl amine (DIPEA, ~ 5 μL). The reaction was stirred at 40°C for 12 hr, at which time it was quenched by the addition of water to precipitate the polymer. The resultant polymer was triturated with hexanes to remove unreacted **2** and dried on vacuum to yield a clear viscous oil in (16 mg, 100% yield). The polymer was analyzed by SEC (0.2% LiBr in DMF): $M_w = 52,000$, $M_n = 43,000$, = 1.20.

Synthesis of cholestanone-terminated poly(glycidyl azide), pGA (4)

The chloride to azide exchange in pECH polymer **3** was accomplished according to previously published procedure.[21] Briefly, in a flame-dried Schlenk flask (10 mL), polymer **3** (15 mg, 0.16 mmol) was dissolved in dry DMF (300 μL). To the solution was added NaN$_3$ (21 mg, 0.32 mmol, 2.0 equiv.), and the reaction was stirred at 60 °C for 3 days under argon to allow complete conversion. Polymer solution was filtered and precipitated in ethanol to yield a clear viscous oil (16 mg, 100 % yield). The polymer was analyzed by SEC (0.2% LiBr in DMF): $M_w = 51,000$, $M_n = 41,800$, = 1.22.

Synthesis of Cy5-labeled glycopolymers 5

In a flame-dried Schlenk flask (10 mL), polymer **4** (9.00 mg, 0.09 mmol) was dissolved in degassed dry DMSO (250 μL). To the solution was added Cy5-alkyne (0.50 mg, 0.50 μmol) in DMSO (50 μL), followed by CuI (2.00 mg, 9.00 μmol) and DIPEA (16 uL, 0.09 mmol). The reaction was stirred in dark under Ar at 40 °C for 2 hrs. After this time, the reaction mixture was aliquoted (50 μL) into separate vials containing β-propargyl glucoside, galactoside, fucoside, and glucuronoside (0.03 mmol, 2.00 equiv. per azide side-chain) in degassed anhydrous DMSO (50 μL). The reactions were stirred in dark at 40°C overnight. After this time, the reactions were diluted with DI water and treated with Cuprisorb beads (SeaChem labs) for 18 hrs to sequester copper. The resulting copper-free solutions were filtered through celite to remove the resin and lyophilized. The dry residues were triturated 3x with methanol with monitoring by TLC to remove excess unreacted glycosides. The resulting Cy5-labeled glycopolymers **5** were dissolved in D_2O and lyophilized to give a blue solid in a quantitative yield for each polymer (*note*: the blue color of the glycopolymers arises from the presence of the Cy5 label and not residual copper contamination. Glycopolymers lacking the Cy5 label were isolated as white solids). The polymers **5** were characterized using ^{1}H NMR (CDCl$_3$, 300 MHz) and UV-Vis (λ_{max} = 633 nm) spectroscopy and analyzed by aqueous SEC. Absorbance readings at known concentrations of glycopolymers **5** indicating the presence of ~ 2 Cy5 molecules per polymer chain (0.5% sidechain occupancy). The resulting glycopolymers were analyzed by aqueous SEC (0.2M NaNO$_3$ in 0.01M Na$_2$HPO$_4$, pH = 7.0). **5 Glc**: $M_{n,calc.}$ = 143 kDa, $M_{n,SEC}$ = 20,578, = 1.369; **5-Gal**: $M_{n,calc.}$ = 143 kDa, $M_{n,SEC}$ = 21,273, = 1.374; **5-Fuc**: $M_{n,calc.}$ = 136 kDa, $M_{n,SEC}$ = 18,562, = 1.306; **5-GlcA**: $M_{n,calc.}$ = 149 kDa, $M_{n,SEC}$ = 31,725, = 2.099.

Remodeling of RBC glycocalyx with glycopolymers 5

RBCs (4% w/v in PBS) were incubated with Cy5-labeled glycopolymers **5** at increasing concentrations (c_{pol} = 0.1–10.0 μM) for 1 h at 37 °C. The cells washed 1x with PBS, then were probed for the presence of Cy5 fluorescence using flow cytometry. The data were analyzed on Cytobank online software. Cells were gated to exclude debris, and the median fluorescence intensities (MFI) of cells are reported. Means and standard deviations for each condition were calculated from three independent biological replicates.

Determination of Cell morphology by Electron Microscopy

RBCs treated with glycopolymers **5** at concentrations of 2.5 μM and 10.0 μM, as well as untreated cells, were prepared fixed in glutaraldehyde solution in PBS (2.5%) at 4 °C overnight. The cells were gradually transferred into EtOH by washes with DI water containing gradually increasing concentrations of EtOH (0–100%, 10% increments). The samples were dried using Tousimis AutoSamdri 815A critical point dryer and sputter coated with Iridium for 8 seconds using Emitech K575X Iridium Sputter coater. SEM imaging was done with ETD detector at HV 4.00KV with 0.1 nA current.

Agglutination of glycocalyx-remodeled RBCs in the presence of ConA and SNA lectins

In a round-bottom 96 well plates containing RBCs (25uL, 1% in PBS) treated with glycopolymers **5** (2.5 μM) or alkynyl cholestanone **2** (2.5 μM), or untreated cells were added

fluorescein-labeled ConA and SNA lectins (25 uL) at increasing concentrations (c_{ConA} = 0 – 1.8 ug/mL and c_{SNA} = 0 – 0.25 ug/mL). The cells were mixed gently but thoroughly using a pipette tip and, then, allowed to agglutinate for 45 min. After this time, the plates were scanned on an EPSON Perfection V700 Photo scanner (Digital ICE technologies), and the lowest lectin concentrations required to induce RBC agglutination were determined. The settling of RBCs to the bottom of a well to form a solid dot shape indicated a lack of agglutination. Each condition was evaluated in three independent biological replicates.

Determination of lectin association with glycocalyx-remodeled RBCs by flow cytometry

In a 96 well round bottom plate, to RBCs (0.33% in PBS) treated with glycopolymers **5** (2.5 μM) or alkynyl cholestanone **2** (2.5 μM), or to untreated cells, were added fluorescein-labeled ConA and SNA lectins at sub-agglutination concentrations (c_{ConA} = 8 ug/mL and c_{SNA} = 1 ug/mL). The cells were vortexed vigorously for ~ 10 s and then analyzed by flow cytometry (Canto II) for the presence of fluorescein signal at discrete time points until saturation lectin binding was observed. The data were analyzed on Cytobank software. Cells were gated to exclude debris, and median fluorescence intensities (MFI) of cells are reported. Means and standard deviations were calculated from two independent biological experiments, and p-values corresponding to each condition vs. untreated RBC control were calculated using 2-way ANNOVA tests with PRISM software. The linear regions of the lectin binding curves were determined (t = 0 – 200 s) and fitted using a linear regression in PRISM software. The slopes designating the initial rates of lectin association and the R^2 values for the linear fits were extracted for each condition and their significance with respect to untreated RBC controls was assessed based on p-values calculated using 1-way ANNOVA tests.

Supplementary Material

Refer to Web version on PubMed Central for supplementary material.

Acknowledgements

References

1. Weinbaum S, Tarbell JM, Damiano ER. Annu. Rev. Bio. Eng 2007, 9, 121–167.
The structure and function of the endothelial glycocalyx layer.

2. Varki A, Gagneux P. Biological Functions of Glycans In: Varki A, Cummings RD, Esko JD, et al., editors. Essentials of Glycobiology 3rd edition Cold Spring Harbor (NY): Cold Spring Harbor Laboratory Press, Chapter 7, 2015–2017.

3. Cummings RD, Schnaar RL, Esko JD, Drickamer K & Taylor ME Principles of Glycan Recognition In: Varki A, Cummings RD, Esko JD, et al., editors. Essentials of Glycobiology 3rd edition Cold Spring Harbor (NY): Cold Spring Harbor Laboratory Press, Chapter 29, 2015–2017.

4. Brewer CF, Miceli MC & Baum LG Clusters, bundles, arrays and lattices: novel mechanisms for lectin–saccharide-mediated cellular interactions. Curr. Opin. Struct. Biol. 2002, 12, 616–623. [PubMed: 12464313]

5. Huang ML & Godula K Nanoscale materials for probing the biological functions of the glycocalyx. Glycobiology 2016, 26, 797–803. [PubMed: 26916883]

6. Bhatia S, Camacho LC & Haag R Pathogen Inhibition by Multivalent Ligand Architectures. J. Am. Chem. Soc. 2016, 138, 8654–8666; [PubMed: 27341003] Mammen M, Choi S-K & Whitesides GM Polyvalent Interactions in Biological Systems: Implications for Design and Use of Multivalent Ligands and Inhibitors. Angew. Chem. Int. Ed. 1998, 37, 2754–2794;Gestwicki JE, Cairo CW, Strong LE, Oetjen KA & Kiessling LL Influencing Receptor–Ligand Binding Mechanisms with Multivalent Ligand Architecture. J. Am. Chem. Soc. 2002, 124, 14922–14933. [PubMed: 12475334]

7. Kiessling LL, Gestwicki JE & Strong LE Synthetic Multivalent Ligands as Probes of Signal Transduction. Angew. Chem. Int. Ed Engl. 2006, 45, 2348–2368. [PubMed: 16557636]

8. Purcell SC & Godula K Synthetic glycoscapes: addressing the structural and functional complexity of the glycocalyx. Interface Focus 2019, 9: 20180080.

9. Rabuka D, Forstner MB, Groves JT, Bertozzi CR Noncovalent Cell Surface Engineering: Incorporation of Bioactive Synthetic Glycopolymers into Cellular Membranes. J. Am. Chem. Soc. 2008, 130, 5947–5953. [PubMed: 18402449]

10. Paszek MJ et al. The cancer glycocalyx mechanically primes integrin-mediated growth and survival. Nature, 2014, 511, 319–325

11. Bradley AJ, Murad KL, Regan KL & Scott MD Biophysical consequences of linker chemistry and polymer size on stealth erythrocytes: size does matter. Biochim. Biophys. Acta BBA - Biomembr. 2002, 1561, 147–158.

12. Chapanian R et al. Influence of polymer architecture on antigens camouflage, CD47 protection and complement mediated lysis of surface grafted red blood cells. Biomaterials, 2012, 33, 7871–7883. [PubMed: 22840223]

13. Siren EMJ, Chapanian R, Constantinescu I, Brooks DE & Kizhakkedathu JN Oncotically Driven Control over Glycocalyx Dimension for Cell Surface Engineering and Protein Binding in the Longitudinal Direction. Sci. Rep. 2018, 8, 7581. [PubMed: 29765073]

14. Hattrup CL & Gendler SJ Structure and Function of the Cell Surface (Tethered) Mucins. Annu. Rev. Physiol. 2008, 70, 431–457. [PubMed: 17850209]

15. Bansil R & Turner BS Mucin structure, aggregation, physiological functions and biomedical applications. Curr. Opin. Colloid Interface Sci. 2006, 11, 164–170.

16. Godula K, Rabuka D, Nam KT & Bertozzi CR Synthesis and Microcontact Printing of Dual End-Functionalized Mucin-like Glycopolymers for Microarray Applications. Angew. Chem. Int. Ed Engl. 2009, 48, 4973–4976. [PubMed: 19479916]

17. Kramer JR, Onoa B, Bustamante C & Bertozzi CR Chemically tunable mucin chimeras assembled on living cells. Proc. Natl. Acad. Sci. 2015, 112, 12574–12579. [PubMed: 26420872]

18. Gervais M, Labbé A, Carlotti S & Deffieux A Direct Synthesis of α-Azido,ω-hydroxypolyethers by Monomer-Activated Anionic Polymerization. Macromolecules, 2009, 42, 2395–2400.

19. Tornøe CW, Christensen C & Meldal M Peptidotriazoles on Solid Phase: [1,2,3]-Triazoles by Regiospecific Copper(I)-Catalyzed 1,3-Dipolar Cycloadditions of Terminal Alkynes to Azides. J. Org. Chem, 2002, 67, 3057–3064.. [PubMed: 11975567]

20. Alarcón-Manjarrez C, Arcos-Ramos R, Álamo MF & Iglesias-Arteaga MA Synthesis, NMR and crystal characterization of dimeric terephthalates derived from epimeric 4,5-seco-cholest-3-yn-5-ols. Steroids, 2016, 109, 66–72 [PubMed: 26968130]

21. Meyer J, Keul H & Möller M Poly(glycidyl amine) and Copolymers with Glycidol and Glycidyl Amine Repeating Units: Synthesis and Characterization. Macromolecules, 2011, 44, 4082–4091.

22. Collins BE et al. Masking of CD22 by cis ligands does not prevent redistribution of CD22 to sites of cell contact. Proc. Natl. Acad. Sci. 2004, 101, 6104–6109. [PubMed: 15079087]

23. Kesimer M et al. Molecular organization of the mucins and glycocalyx underlying mucus transport over mucosal surfaces of the airways. Mucosal Immunol. 2013, 6, 379–392.

24. Hudak JE, Canham SM, Bertozzi CR Glycocalyx engineering reveals a Siglec-based mechanism for NK cell immunoevasion. Nat. Chem. Biol. 2013, 10, 69–75.

25. Gandhi JG, Koch DL & Paszek MJ Equilibrium Modeling of the Mechanics and Structure of the Cancer Glycocalyx. Biophys. J. 2019, 116, 694–708. [PubMed: 30736980]

26. Hudak JE & Bertozzi CR Glycotherapy: New Advances Inspire a Reemergence of Glycans in Medicine. Chem. Biol. 2014, 21, 16–37. [PubMed: 24269151]

27. Liang C-H, Wang S-K, Lin C-W, Wang C-C, Wong C-H, Wu C-Y. Effects of Neighboring Glycans on Antibody-Carbohydrate Interaction. Angew. Chem. Int. Ed. 2011, 50, 1608–1612.

28. Shivatare VS, Shivatare SS, Lee C-CD, Liang CH, Liao K-S, Cheng Y-Y, Saidachary G, Wu C-Y, Lin N-H, Kwong PD, Burton DR, Wu C-Y, Wong C-H. Unprecedented Role of Hybrid N-Glycans as Ligands for HIV-1 Broadly Neutralizing Antibodies. J. Am. Chem. Soc. 2018, 140, 5202–5210 [PubMed: 29578688]

29. Cohen M, Hurtado-Ziola N & Varki A ABO blood group glycans modulate sialic acid recognition on erythrocytes. Blood, 2009, 114, 3668–3676. [PubMed: 19704115]

30. Cohen M and Varki A Modulation of Glycan Recognition by Clustered Saccharide Patches In International Review of Cell and Molecular Biology, Vol. 308, Burlington: Academic Press, 2014, pp. 75–125.

31. Morotti ALM, Lang KL, Carvalho I, Schenkel EP & Bernardes LSC Semi-Synthesis of new glycosidic triazole derivatives of dihydrocucurbitacin B. Tetrahedron Lett. 2015, 56, 303–307.

32. Manabe Y et al. Development of α1,6-fucosyltransferase inhibitors through the diversity-oriented syntheses of GDP-fucose mimics using the coupling between alkyne and sulfonyl azide. Bioorg. Med. Chem. 2017, 25, 2844–2850. [PubMed: 28284868]

33. Sharma DK et al. Ammonium chloride mediated synthesis of alkyl glycosides and evaluation of their immunomodulatory activity. RSC Adv. 2013, 3, 11450–11455.

34. Izawa K & Hasegawa T Tosylated and azided inulins as key substrates for further chemical modifications to access inulin-based advanced materials: An inulin-based glycocluster. Bioorg. Med. Chem. Lett. 2012, 22, 1189–1193. [PubMed: 22177083]
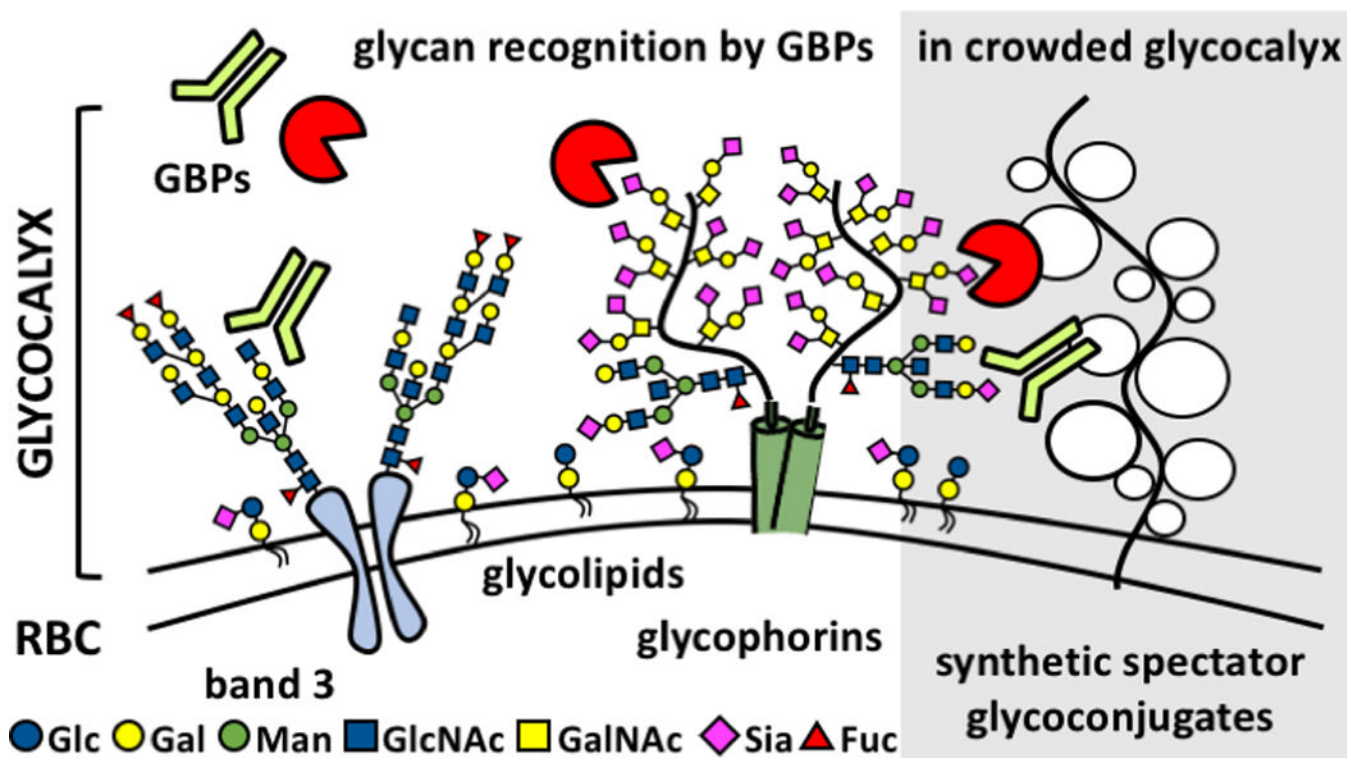
Figure 1.
Recognition of glycans by protein receptors occurs in the dynamic and compositionally heterogeneous environment of the cellular glycocalyx. These interactions can be influenced by the presence and physical properties of non-binding, spectator, glycoconjugates. Synthetic mimetics of membrane associated glycoproteins, such as mucins, can be generated and installed into the native glycocalyx to evaluate how changes in glycocalyx crowding and physical properties impact ligand-receptor interactions.
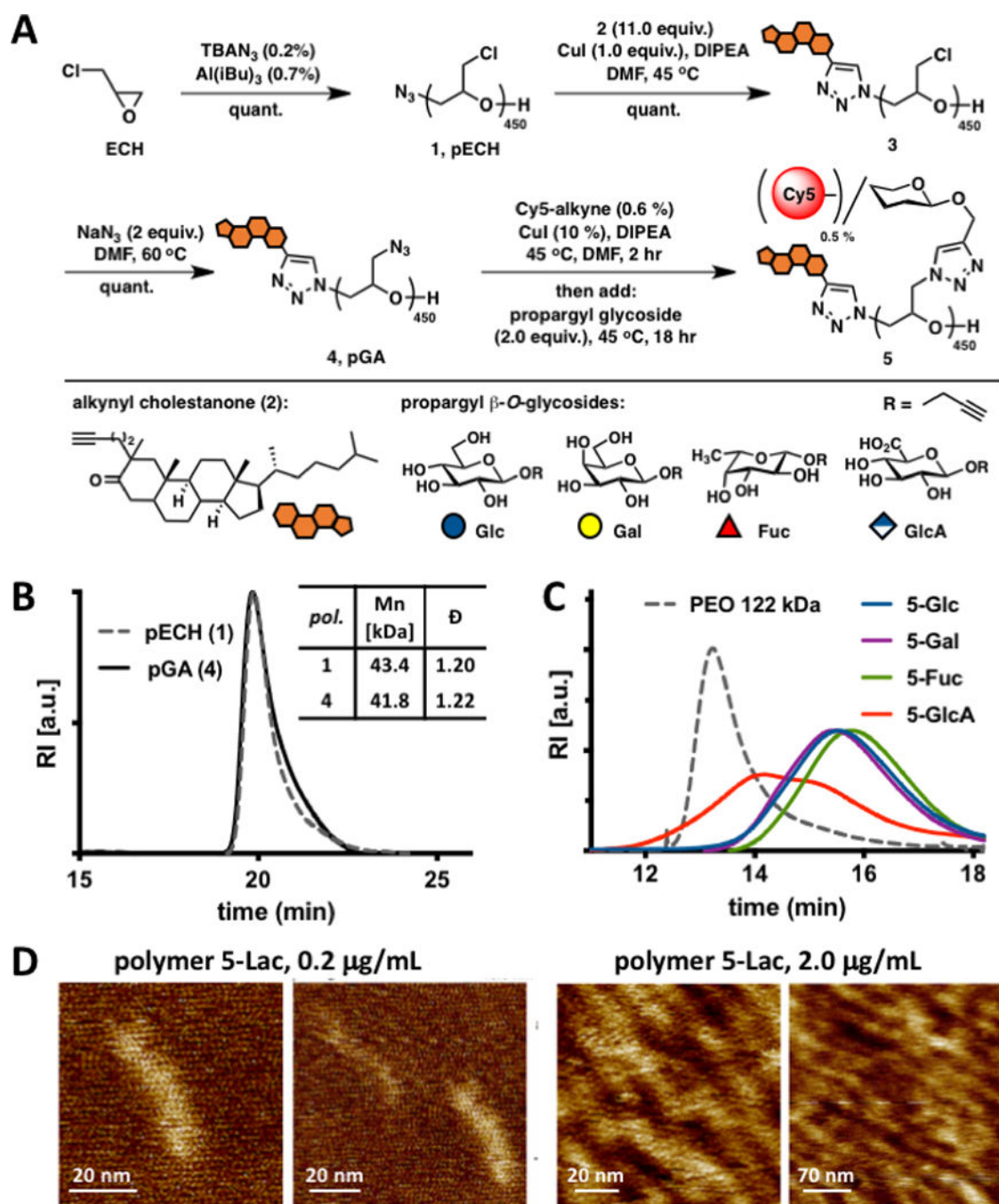
Figure 2.

Synthesis and characterization of mucin mimetics **5**. (A) Glycopolymers **5** were generated from poly(epichlorohydrin) **1** via chloride-to-azide sidechain substitution followed by the CuAAC conjugation of propargyl β-*O*-glycosides (Glc, Gal, Fuc, and GlcA). The polymers were furnished with a hydrophobic cholestanone moiety for anchoring into cell membranes and a Cy5 fluorescent tag for imaging and quantification. (B) SEC analysis indicated narrow molecular weight and chain-length distributions before and after the chloride-to-azide exchange. (C) Glycopolymers **5** exhibited increased retention in aqueous SEC compared to a

PEO standard of similar molecular weight (122 kDa), a characteristic behavior of glycopolymers with extended molecular conformations. (D) AFM imaging of lactose-modified glycopolymers confirmed elongated, mucin-like morphology of the PEG-based glycopolymers.
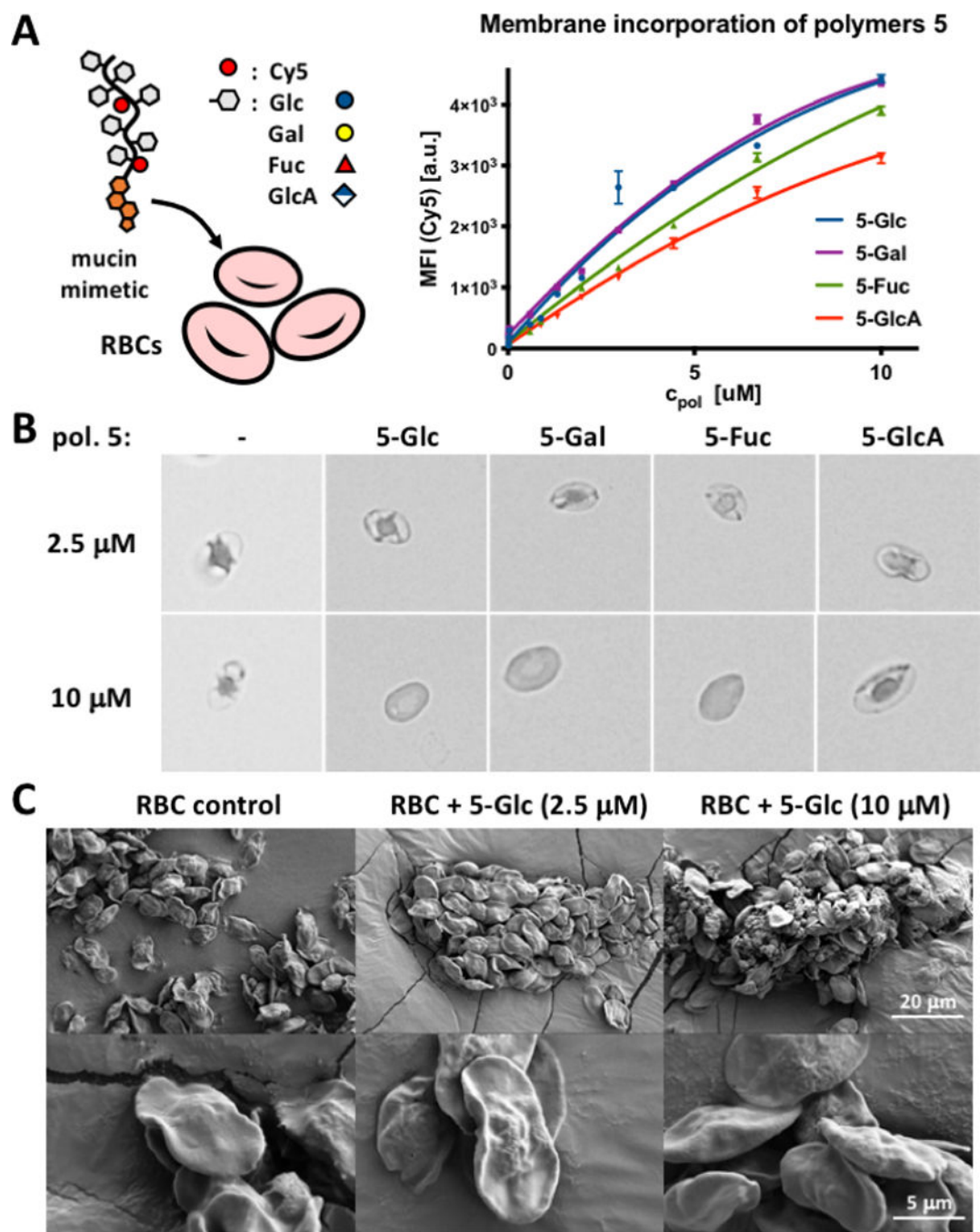
Figure 3.

RBC glycocalyx remodeling with glycopolymers **5**. (A) Polymers **5** incorporate dose-dependently into RBC membranes according to their pendant glycans. Increasing glycopolymer density in RBC membranes induces cell rounding, swelling, and lysis at polymer concentrations above 2.5 uM via brightfield microscopy (B) or SEM (C).
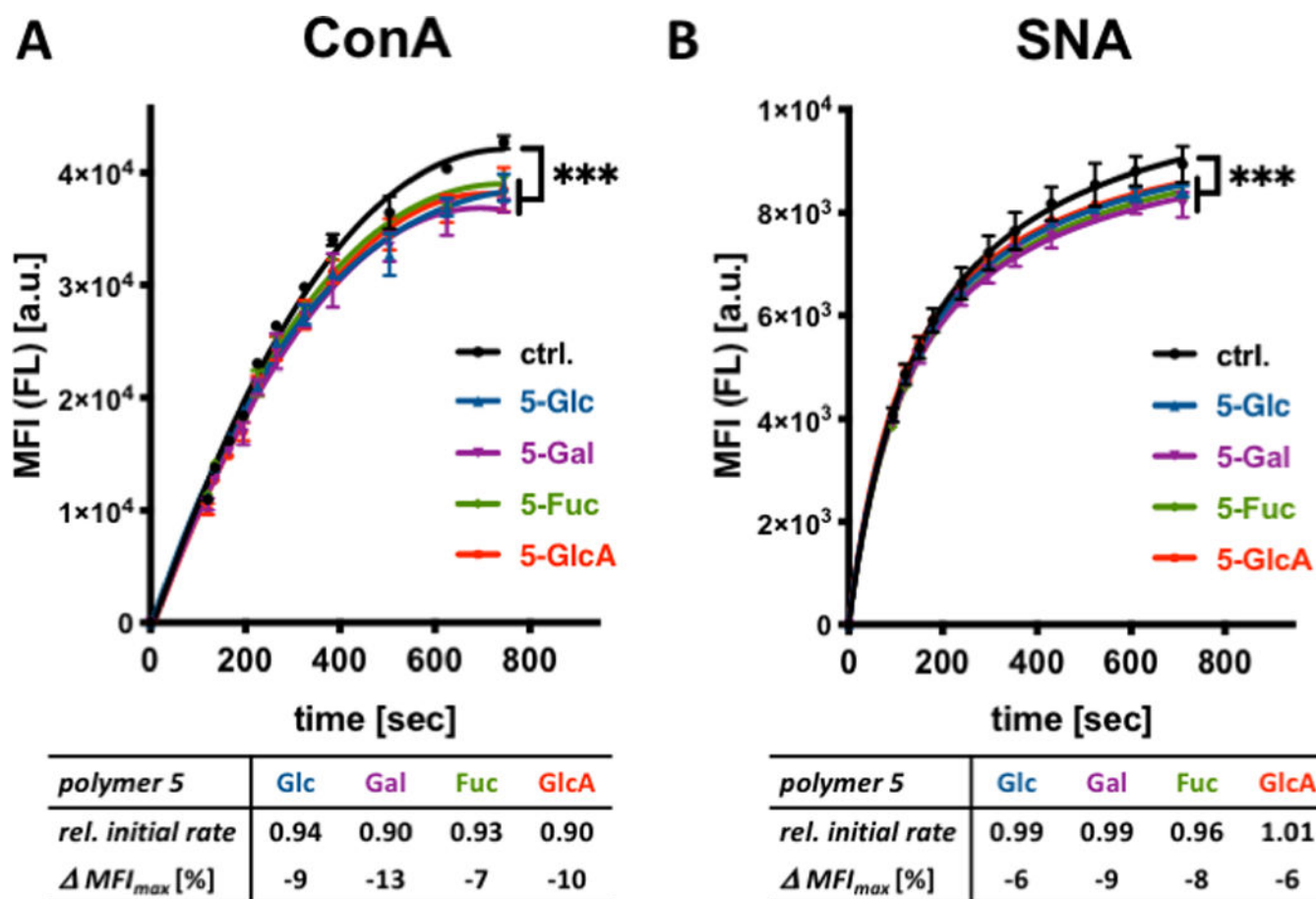
polymer 5	Glc	Gal	Fuc	GlcA
rel. initial rate	0.94	0.90	0.93	0.90
ΔMFI_{max} [%]	-9	-13	-7	-10

polymer 5	Glc	Gal	Fuc	GlcA
rel. initial rate	0.99	0.99	0.96	1.01
ΔMFI_{max} [%]	-6	-9	-8	-6

Figure 4.
Association of ConA and SNA lectins with glycocalyx-remodeled RBCs. (A) Binding of fluorescein (FL)-labeled lectins to remodeled cells were assessed via flow cytometry. The presence of spectator glycopolymers **5** at the surface of RBCs attenuates both the initial rate as well as saturation binding of ConA to cell surface glycans. (B) Glycopolymers **5** have no effect on the initial rates of SNA binding but inhibit lectin association near saturation. Relative initial rates were calculated from the linear regions of lectin binding curves and normalized to control cells without polymer treatment. MFI$_{max}$ corresponds to the change in median fluorescence intensity of cells at saturation lectin binding. (ANOVA, Tukey's multiple comparisons test; $p^{***} < 0.001$).
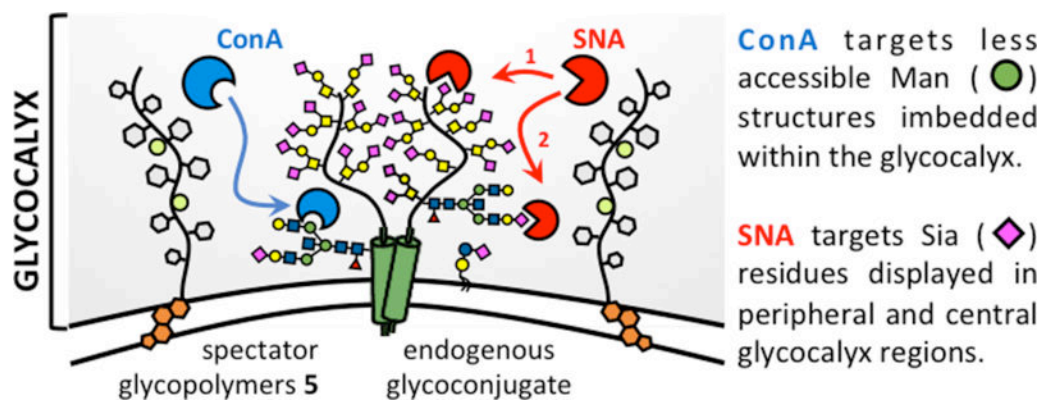
ConA targets less accessible Man (●) structures imbedded within the glycocalyx.

SNA targets Sia (◆) residues displayed in peripheral and central glycocalyx regions.

Figure 5.
Glycocalyx crowding with spectator glycoconjugates differentially affects the association of ConA and SNA with endogenous glycans depending on their distribution throughout the glycocalyx. The glycopolymer spectators inhibit both the initial rates and saturation binding of ConA to the less accessible mannose structures. Glycocalyx crowding influences the association of SNA with sialic acid residues only at later time points near saturation binding, once the more available peripheral glycans have become occupied.

Table 1.

Agglutination of RBCs remodeled with glycopolymers **5** (2.5 uM) by ConA (0 – 1.8 μg/mL) and SNA (0–105 ng/mL) lectins.

	ConA							SNA								
C_ConA [μg/mL]	0 - 0.43	0.57	0.76	1.00	1.30	1.80	C_SNA [ng/mL]	0 - 25	33	45	60	80	105	140	187	250
glycopolymer 5 —		●───	───	───	───	───●	glycopolymer 5 —	●──	──	──	──	──	──	──	──	──●
Glc				●──	──	──●	Glc				●──	──	──	──	──	──●
Gal					●──	──●	Gal							●──	──	──●
Fuc					●──	──●	Fuc							●──	──	──●
GlcA						●─●	GlcA								●──	──●